Fabrication of high quality factor lithium niobate double-disk using a femtosecond laser

Zhiwei Fang, Ni Yao, Min Wang, Jintian Lin, Jianhao Zhang, Rongbo Wu, Lingling Qiao, Wei Fang, Tao Lu, and Ya Cheng

2017

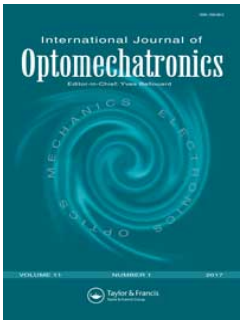

International Journal of Optomechatronics

ISSN: 1559-9612 (Print) 1559-9620 (Online) Journal homepage: http://www.tandfonline.com/loi/uopt20

Fabrication of high quality factor lithium niobate double-disk using a femtosecond laser

Zhiwei Fang, Ni Yao, Min Wang, Jintian Lin, Jianhao Zhang, Rongbo Wu, Lingling Qiao, Wei Fang, Tao Lu & Ya Cheng

To cite this article: Zhiwei Fang, Ni Yao, Min Wang, Jintian Lin, Jianhao Zhang, Rongbo Wu, Lingling Qiao, Wei Fang, Tao Lu & Ya Cheng (2017) Fabrication of high quality factor lithium niobate double-disk using a femtosecond laser, International Journal of Optomechatronics, 11:1, 47-54, DOI: 10.1080/15599612.2017.1406024

To link to this article: https://doi.org/10.1080/15599612.2017.1406024

Published online: 19 Dec 2017.

INTERNATIONAL JOURNAL OF OPTOMECHATRONICS
2017, VOL. 11, NO. 1, 47–54
https://doi.org/10.1080/15599612.2017.1406024

Fabrication of high quality factor lithium niobate double-disk using a femtosecond laser

Zhiwei Fang[a,b,c], Ni Yao[d], Min Wang[a,b], Jintian Lin[a], Jianhao Zhang[a,b], Rongbo Wu[a,b], Lingling Qiao[a], Wei Fang[d], Tao Lu[e], and Ya Cheng[a,f,g]

[a]State Key Laboratory of High Field Laser Physics, Shanghai Institute of Optics and Fine Mechanics, Chinese Academy of Sciences, Shanghai, P. R. China; [b]University of Chinese Academy of Sciences, Beijing, P. R. China; [c]School of Physical Science and Technology, ShanghaiTech University, Shanghai, P. R. China; [d]State Key Laboratory of Modern Optical Instrumentation, College of Optical Science and Engineering, Zhejiang University, Hangzhou, P. R. China; [e]Department of Electrical and Computer Engineering, University of Victoria, Victoria, Canada; [f]State Key Laboratory of Precision Spectroscopy, East China Normal University, Shanghai, P. R. China; [g]Collaborative Innovation Center of Extreme Optics, Shanxi University, Taiyuan, P. R. China

ABSTRACT

We demonstrate fabrication of a high-quality factor lithium niobate double-disk whispering-gallery microcavity using femtosecond laser assisted ion beam milling. Using this method, two vertically stacked 30-μm diameter disks with a 200-nm gap are fabricated. With our device, an optical quality factor as high as 1.35×10^5 is demonstrated. Our approach is scalable to fabricate multiple disks on a single chip.

KEYWORDS

Double disk; integrated optics; lithium niobate; microfabrication; microresonator

1. Introduction

High-quality (Q) factor whispering-gallery microcavities (WGMs) have attracted much attention for their broad range of applications ranging from optical signal processing and cavity quantum electrodynamics to biosensing and optomechanics.[1–10] Currently, high-Q WGMs are mostly fabricated using conventional chemical etching techniques with e-beam or photo lithography, thermal reflow as well as mechanical milling and polishing technologies.[11–13] The mechanical approach lacks the potential for monolithic integration of multiple WGMs for on-chip applications while the choice of etchant and reflow ones are limited by materials used in WGMs. For example, silica microspheres are conventionally fabricated by reflowing fiber tips using a CO_2 laser as silica strongly absorbs the energy of 10-μm wavelength light emitted by such laser. Fabricating a CaF_2 microsphere must take other approaches such as mechanical polishing since such material is transparent at the infrared wavelength. In fabricating silica or $LiNbO_3$ microdisks, HF acid is used as the etchant while a different etchant such as XeF_2 or SF_6 is required for silicon cavity fabrication. Therefore, developing efficient fabrication techniques for producing on-chip crystalline WGMs is still challenging due to the incompatibility of a large number of crystalline materials and optical lithography. Nevertheless, it has recently been shown that femtosecond laser micromachining provides a promising approach to fabricating high-Q WGMs on various materials including glasses,[14–16] polymers,[17,18] and crystals.[19–21] It is noteworthy that the successful demonstrations of high-Q WGMs on crystalline substrates open the door for miniaturized nonlinear optics applications.

CONTACT Ya Cheng ya.cheng@siom.ac.cn No. 390 Qinghe Road, Jiading, Shanghai 201800, China;
Tao Lu taolu@ece.uvic.ca EOW 448, 3800 Finnerty Rd., Victoria, BC V8P 5C2, Canada.
Color versions of one or more of the figures in the article can be found online at www.tandfonline.com/uopt.

Nomenclature

WGMs	whispering-gallery microcavities	NA	numerical aperture
high-Q	high-quality	HF	hydrofluoric
Q factor	quality factor	SEM	scanning electron microscope
LN	lithium niobate	FSR	free spectral range
FIB	focused ion beam	QED	quantum electrodynamics

In the past few years, significant nonlinear optical phenomena and efficient electro-optic tuning effects have been experimentally demonstrated in lithium niobate (LN) WGMs.[22–26] In addition, the capability of monolithic integration of LN microresonators with various nanophotonic structures has been reported.[25–27] To date, only single-layered LN microdisks have been fabricated using the LN thin film substrate. It is known that silica double-disk is one of the unique structures which displays strong optomechanical effects due to the large optical gradient force provided by the strong interaction of optical fields between the top and bottom disks.[28–32] Here, we fabricate double-disks on LN platform by utilizing a femtosecond laser in combination with focused ion beam (FIB) as the LN crystal has advantageous nonlinear optical, mechanical and electro-optical properties compared to SiO_2. The unique physical properties of LN can influence the optomechanical responses in WGMs and in turn provide opportunities to new findings and applications.

2. Experiment

We designed the double-layer X-cut LN thin film substrate as illustrated in Figure 1(*a*). The top and bottom LN thin films of 300 nm in thickness, respectively, are separated by a thin layer of SiO_2 with a thickness of 200 nm. The double-layer LN thin film is bonded to a 2-μm thick SiO_2 substrate, which is bonded to the 500-μm thick LN substrate. Following our design, the wafer was produced by NANOLN, Jinan Jingzheng Electronics Co., Ltd. A Ti:sapphire femtosecond laser source (Coherent, Inc., center wavelength: 800 nm, pulse width: 40 fs, repetition rate: 1 kHz) was used for fabricating the on-chip double-disk LN microresonator. In the femtosecond laser direct writing process, a variable neutral density filter was used to tune the average power of the laser beam, and the femtosecond laser pulse energy is adjusted to 3 μJ. An objective lens (100×/NA 0.80) was used to focus the beam down to a ~1 μm-diameter focal spot. The sample could be arbitrarily translated in 3D space at a resolution of 1 μm using a PC-controlled XYZ stage combined with a nanopositioning stage. A charged coupled device connected to the computer was installed to monitor the fabrication process in real time.

The procedures of fabricating the LN double-disk WGM are schematically illustrated in Figure 1. First, the LN substrate was immersed in water and ablated with tightly focused femtosecond laser pulses, as shown in Figure 1(*a*). The ablation in water can help reduce the debris and cracks in the fabricated structure. The height of the cylindrical microstructure patterned with femtosecond laser ablation is ~5 μm, as shown in Figure 1(*b*). The femtosecond laser fabrication took about 1 h. Next, the periphery of the LN double-disk WGM were smoothed using FIB milling, as illustrated in Figure 1(*c*). In the FIB milling, a 30-kV ion beam with a beam current of 1 nA was used. The FIB milling was completed in 10 min. Finally, chemical wet etching, which selectively removes the SiO_2 layers underneath the LN thin films to form free-standing double LN microdisks, was performed in a solution of 2% hydrofluoric (HF) for 8 min, as shown in Figure 1(*e*). The SiO_2 layer was partially preserved to support the double-disk LN microresonator. The diameter of the LN microdisk is 30 μm. It took about 1.5 h in total to produce the LN double-disk WGM.

3. Measurement of quality factor and analysis of WGM modes

The optical micrograph in Figure 2(*a*) shows the top-view image of the fabricated LN double-disk WGM. The side-view image obtained with the scanning electron micrograph (SEM) is presented

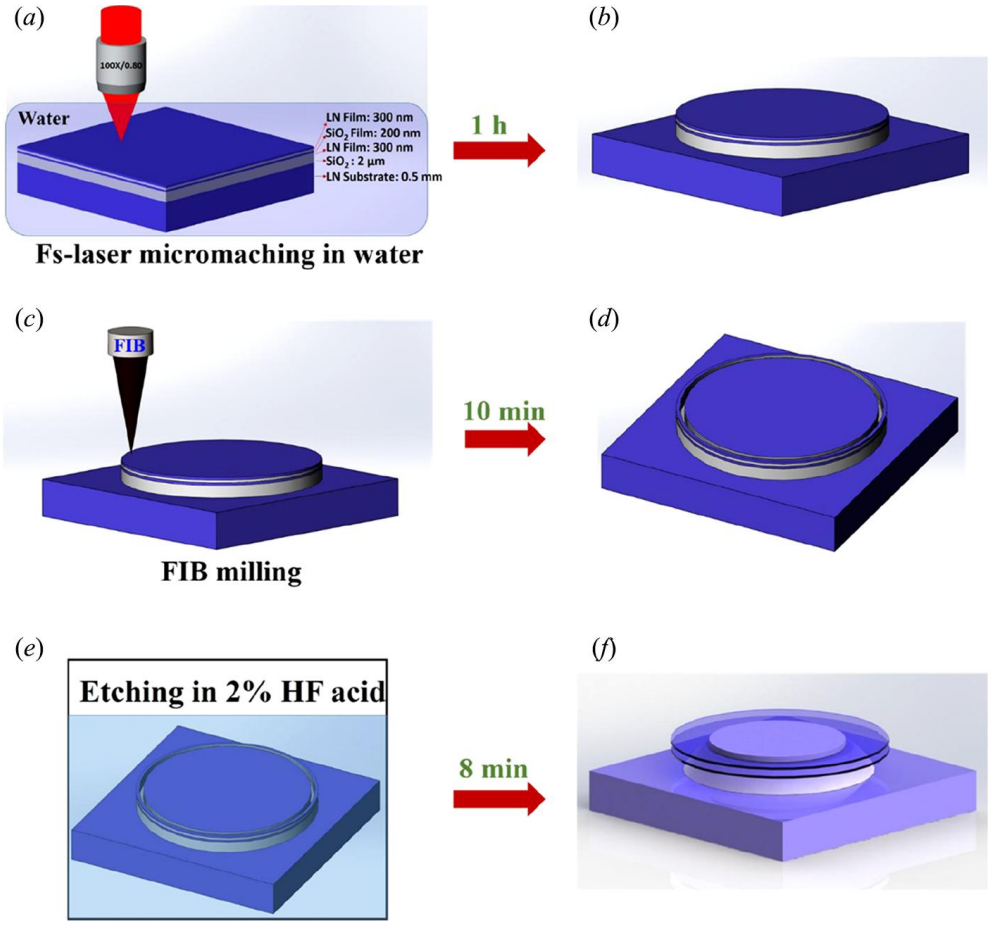

Figure 1. The processing flow of fabricating an on-chip LN double-disk WGM. (*a*) Fabrication of the LN double-disk WGM using femtosecond laser microfabrication. (*b*) The structure obtained after the laser fabrication. (*c*) Focused ion beam (FIB) milling to smooth the periphery of the LN double-disk WGM. (*d*) The structure obtained after the FIB milling. (*e*) Chemical wet etching of the sample undergone the FIB milling to form the freestanding LN double-disk WGM. (*f*) The structure obtained after the chemical wet etching. *Note*: WGM, whispering-gallery microcavity.

in Figure 2(*b*), which reveals the detailed geometry of the fabricated LN double-disk. From the right inset in Figure 2(*b*), we determine that the thicknesses of top and bottom LN disks are 291 and 312 nm, respectively. An air gap of 138 nm is created between the top and bottom disks after the silica layer is partially removed by the chemical etching. In particular, from the left inset in Figure 2(*b*), the

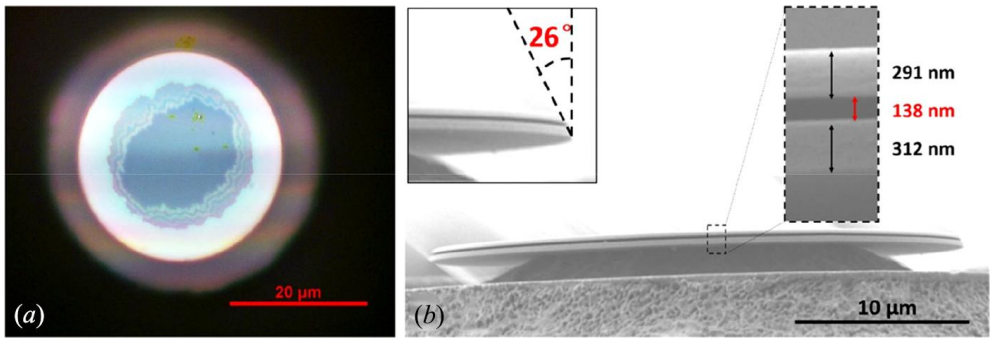

Figure 2. (*a*) Top view optical micrograph and (*b*) side view SEM image of the 30-μm LN double-disk WGM fabricated with femtosecond laser micromachining combined with FIB milling. *Note*: SEM, scanning electron micrograph; WGM, whispering-gallery microcavity; FIB, focused ion beam.

sidewall of the double-disk displays a tilt angle of 26° with respect to the axis perpendicular to the double-disk plane (Figure 2(*b*)). This slanting sidewall is caused by the conical ion beam used in the milling process. The surface appears smooth under the SEM examination, which ensures a high-*Q* factor of the fabricated double-disk as we have demonstrated before.[21]

To measure the *Q* factor of the fabricated LN double-disk WGM, we used a system as shown in Figure 3. Here, a narrow-bandwidth continuous-wave tunable diode laser (New Focus, Model 688-LN) was used as the light source. The tunable laser has a linewidth of 10 MHz in frequency, a spectral tuning range from 1510 to 1620 nm and a power of about 1 mw. The wavelength-tunable light was first coupled into and then extracted from the microdisk through a tapered optical fiber. A transient photo detector (Lafayette, Model 4650) was connected to the output of the tapered fiber for measuring the transmission spectrum. The WGM modes of quasi-TE polarization states were selectively excited using an in-line fiber polarization controller.

Figure 4(*a*) shows the measured transmission spectrum of a fabricated LN double-disk. As shown in the plot, a free spectral range (FSR) of 11.9 nm is observed. This is in close agreement with our simulated FSR of 12.5 nm. The zoom-in spectrum at 1528.45 nm is shown in Figure 4(*b*) where mode splitting is observed. Based on a Lorentzian fitting, the *Q* factors of the splitting modes were determined to be 1.35×10^5 and 1.21×10^5.[33] Another zoom-in spectrum shown in Figure 4(*c*) further displays a single resonance mode with *Q* of 1.06×10^5 at 1552.20 nm. The result clearly shows that our LN double-disk can have a high *Q* factor on the same level of that of single-disk LN microresonator.

Furthermore, we attempted to identify some of the modes with numerical simulations. Figure 5(*a*) shows a recorded transmission spectrum of another LN disk at 1573.22 nm (i.e., the black curve), from which an overall optical *Q*-factor of 1.2×10^5 can be determined with Lorentz fitting curve in red. Here, a full vector WGM mode solver was implemented using COMSOL 2D axisymmetric, wave optics frequency domain electromagnetics module. In this simulation, we assume the refractive index of LN to be $2.2111 + 2.467 \times 10^{-8}i$.[34] The edge of the double disk is centered in an 8-μm wide and 3-μm high computation window. To minimize the spurious reflection, 1.55-μm thick perfect match layers were added at the edges of the window. The inset in Figure 5(*a*) shows the simulated WGM profile in the double disk, which corresponds to the fundamental quasi-TE mode at an azimuthal order of 102 at a resonance wavelength of 1572.16 nm. The resonant wavelengths obtained from experimental measurement and simulation nicely agree with each other, indicating that the measured mode is highly likely to be the mode shown in the inset. The slight difference in resonance wavelengths between the experiment and simulation can be attributed to the perturbation from the fiber taper, which can be modeled through perturbation[35] or mode matching methods.[36,37] We note that due to the existence of high-order modes and lack of full geometric information of the double-disk microcavity, complete determination of the modes by measurements requires more

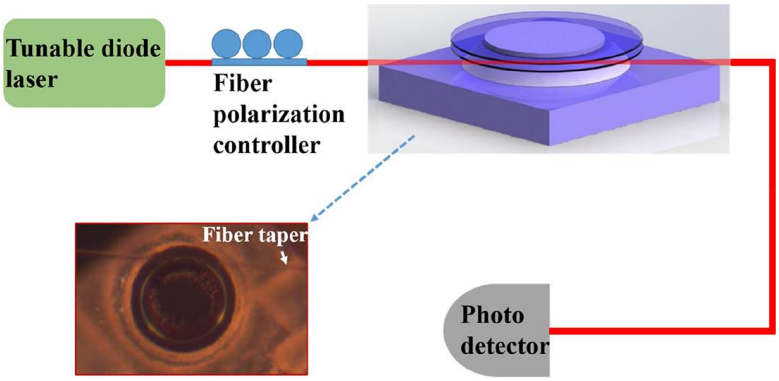

Figure 3. Experimental setup for recording the transmission spectra of the LN double-disk WGM. *Note*: WGM, whispering-gallery microcavity.

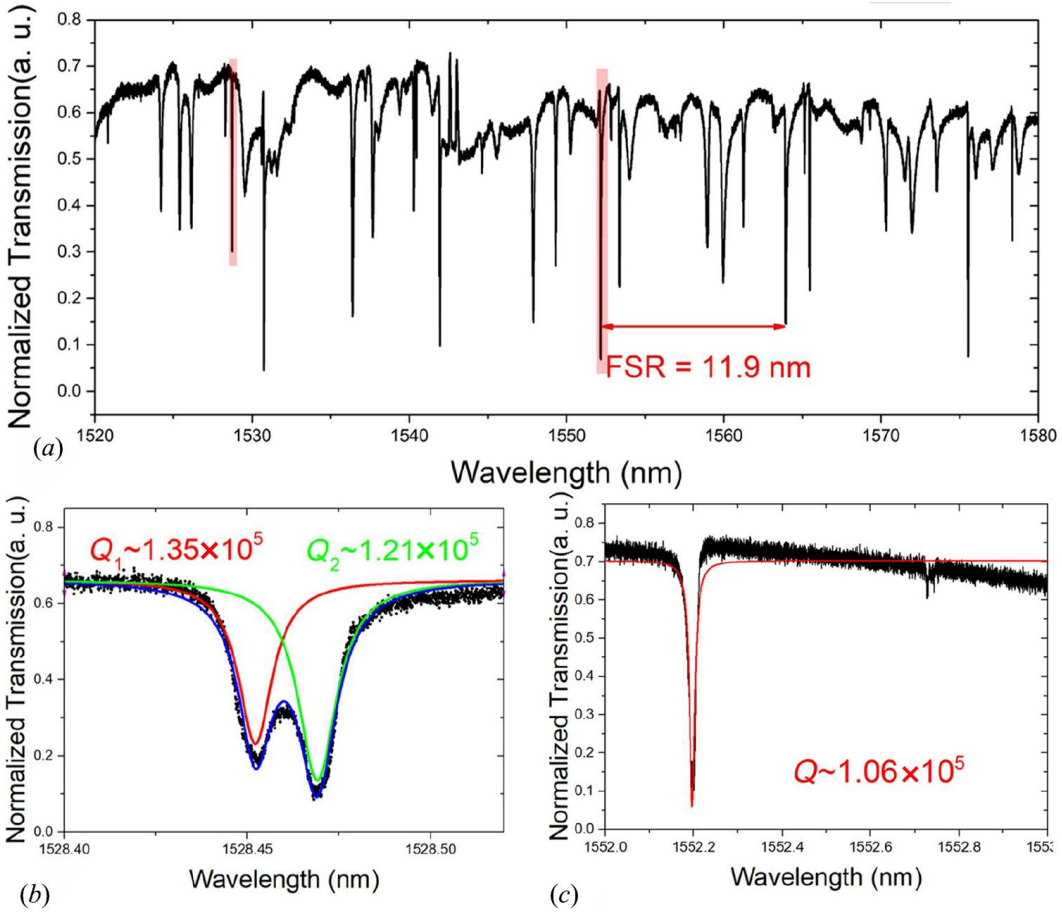

Figure 4. (*a*) Normalised transmission spectrum of the LN double-disk. The Lorentzian fittings showing (*b*) mode splitting with two similar *Q*-factors of 1.35 × 10^5 and 1.21 × 10^5 as measured around 1528.45 nm, and (*c*) a *Q*-factor of 1.06 × 10^5 as measured at 1552.20 nm.

sophisticated techniques, which will be practiced in the future. The simulation also indicated an optical *Q* of 4.8 × 10^7 after only considering the absorption loss, corresponding to the ultimate *Q* value of such devices after optimizing our fabrication processes (i.e., by suppressing the scattering loss at the sidewalls as much as possible).

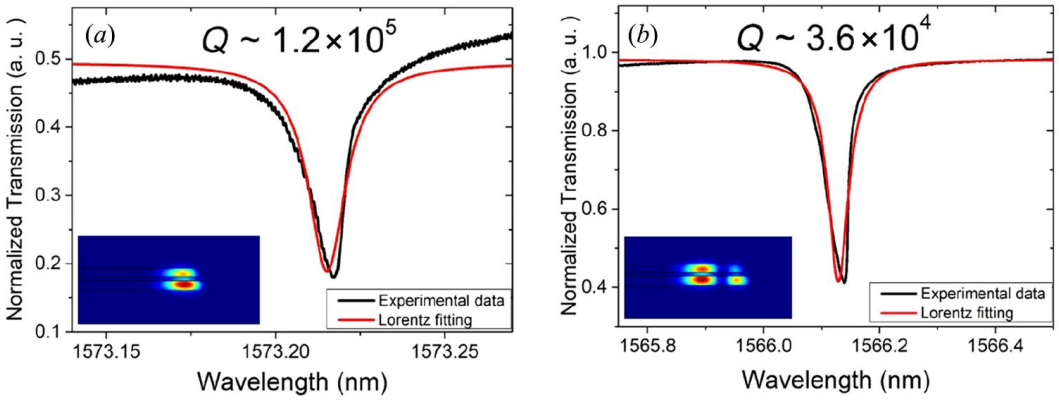

Figure 5. *Q*-factors of (*a*) 1.2 × 10^5 measured at 1573.22 nm and (*b*) 3.6 × 10^4 measured at 1566.13 nm. The corresponding mode profiles revealed by the simulations are shown in the insets.

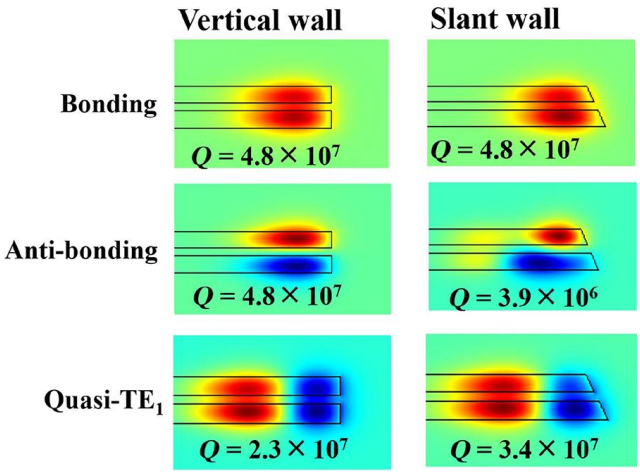

Figure 6. Electrical field distributions of different modes along the radial direction. The type of mode is indicated next to the mode. The left column: vertical sidewall. The right column: slant sidewall. The parameters used in the simulations are given in the text.

Furthermore, Figure 5(*b*) shows another measured *Q*-factor of 3.6×10^4 at 1566.13 nm, which is derived from Lorentz fitting as well. According to the simulation, the experimentally observed mode in Figure 5(*b*) may be attributed to a high order transverse mode at an azimuthal order of 96 with a resonance wavelength of 1565.91 nm. In contrast to the result reported in Lin et al.[29] our simulations show that the 64° wedge angle leads to degradation of *Q* for antibond modes by an order of magnitude. For illustration, we have also conducted a set of comparative simulations on two types of double disks with either a vertical or a slant wall. Here, the simulation parameters of both disks are the same as in Figure 5 except for the wedge angles. As shown in Figure 6, when the disk edge is vertical, the antibonding mode has a *Q* similar to the bonding mode. This is consistent with previously published results.[29] However, our device displayed a slant edge as shown in Figure 2. As indicated by our simulation results in Figure 6, this will degrade *Q* by an order of magnitude, much lower than the higher-order mode displayed in the inset of Figure 5(*b*). Since higher *Q* modes are easier to be excited, we believe that the mode we observed is more likely to be the higher-order mode while the antibond mode was unlikely to be excited in our LN double-disk structure.

4. Conclusion

To conclude, we have demonstrated fabrication of LN double-disks of *Q* factors on the order of 10^5. Our technique combines femtosecond laser direct writing and FIB milling, thereby providing both high fabrication efficiency and ultra-high fabrication resolution. We envisage that such device is an excellent platform for the study of cavity quantum electrodynamics (QED) where the LN provides another dimension of control to the corresponding experiments. In future researches, we will exploit the unique electro-optical and nonlinear optical properties of such device to provide the tunability for investigating cavity optomechanics and nonlinear optics.[26] For example, we can electrically control the refractive index of LN microcavity in real-time for tuning or locking optomechanical frequency. The strong nonlinear effects displayed from LN further enable us to study the intriguing interplay between optomechanics and nonlinear optical phenomenon.

Acknowledgments

Tao Lu would like to acknowledge Natural Sciences and Engineering Research Council of Canada (NSERC) Discovery (RGPIN-2015-06515) and CMC Microsystems.

Funding

National Basic Research Program of China (Program 973, 2014CB921300), Natural National Science Foundation of China (NSFC; 61590934, 61505231, 61405220, 61327902, and 61590934), the Fundamental Research Funds for the Central Universities, and the Open Fund of the State Key Laboratory on Integrated Optoelectronics (IOSKL2015KF34).

References

[1] Vahala, K. J. Optical Microcavities. *Nature* **2006**, *424*, 839–846.
[2] Kippenberg, T. J.; Spillane, S. M.; Vahala, K. J. Kerr-Nonlinearity Optical Parametric Oscillation in an Ultrahigh-Q Toroid Microcavity. *Phys. Rev. Lett.* **2004**, *93*, 083904.
[3] Aoki, T., Dayan, B.; Wilcut, E.; Bowen, W. P.; Parkins, A. S.; Kippenberg, T. J.; Vahala, K. J.; Kimble, H. J. Observation of Strong Coupling Between One Atom and a Monolithic Microresonator. *Nature* **2006**, *443*, 671–674.
[4] Lu, T., Lee, H.; Chen, T.; Herchak, S.; Kim, J.-H.; Fraser, S. E.; Flagan, R. C.; Vahala, K. J. High Sensitivity Nanoparticle Detection Using Optical Microcavities. *Proc. Natl. Acad. Sci. U. S. A* **2011**, *108*, 5976–5979.
[5] Yu, W.; Jiang, W. C.; Lin, Q.; Lu, T. Cavity Optomechanical Spring Sensing of Single Molecules. *Nat. Commun.* **2016**, *7*, 12311.
[6] Kippenberg, T. J.; Vahala, K. J. Cavity Optomechanics: Back-Action at the Mesoscale. *Science* **2008**, *321*, 1172–1176.
[7] Aspelmeyer, M.; Kippenberg, T. J.; Marquardt, F. Cavity Optomechanics. *Rev. Mod. Phys.* **2014**, *86*, 1391.
[8] Fan, X.; White, I. M.; Shopova, S. I.; Zhu, H.; Suter, J. D.; Sun, Y. Sensitive Optical Biosensors for Unlabeled Targets: A Review. *Anal. Chim. Acta* **2008**, *620*, 8.
[9] Dantham, V. R.; Holler, S.; Barbre, C.; Keng, D.; Kolchenko, V.; Arnold, S. Label-Free Detection of Single Protein Using a Nanoplasmonic-Photonic Hybrid Microcavity. *Nano Lett.* **2013**, *13*, 3347.
[10] Baaske, M. D.; Foreman, M. R.; Vollmer, F. Single-Molecule Nucleic Acid Interactions Monitored on a Label-Free Microcavity Biosensor Platform. *Nat. Nanotechnol.* **2014**, *9*, 933.
[11] Armani, D. K.; Kippenberg, T. J.; Spillane, S. M.; Vahala, K. J. Ultra-High-Q Toroid Microcavity on a Chip. *Nature* **2003**, *421*, 925.
[12] Savchenkov, A. A.; Ilchenko, V. S.; Matsko, A. B.; Maleki, L. Kilohertz Optical Resonances in Dielectric Crystal Cavities. *Phys. Rev. A* **2004**, *70*, 051804.
[13] Fürst, J. U.; Strekalov, D. V.; Elser, D.; Lassen, M.; Andersen, U. L.; Marquardt, C.; Leuchs, G. Naturally Phase-Matched Second-Harmonic Generation in a Whispering-Gallery-Mode Resonator. *Phys. Rev. Lett.* **2010**, *104*, 153901.
[14] Lin, J.; Yu, S.; Ma, Y.; Fang, W.; He, F.; Qiao, L.; Tong, L.; Cheng, Y.; Xu, Z. On-Chip Three-Dimensional High-Q Microcavities Fabricated by Femtosecond Laser Direct Writing. *Opt. Express* **2012**, *20*, 10212–10217.
[15] Lin, J.; Xu, Y.; Song, J.; Zeng, B.; He, F.; Xu, H., Sugioka, K.; Fang, W.; Cheng, Y. Low-Threshold Whispering-Gallery-Mode Microlasers Fabricated in a Nd: Glass Substrate by Three-Dimensional Femtosecond Laser Micromachining. *Opt. Lett.* **2013**, *38*, 1458–1460.
[16] Tielen, V.; Bellouard, Y. Three-Dimensional Glass Monolithic Micro-Flexure Fabricated by Femtosecond Laser Exposure and Chemical Etching. *Micromachines* **2014**, *5*, 697–710.
[17] Liu, Z. P.; Li, Y.; Xiao, Y. F.; Li, B. B.; Jiang, X. F.; Qin, Y.; Feng, X. B.; Gong, Q. Direct Laser Writing of Whispering Gallery Microcavities by Two-Photon Polymerization. *Appl. Phys. Lett.* **2010**, *97*, 211105.
[18] Zhan, X. P.; Ku, J. F.; Xu, Y. X.; Zhang, X. L.; Zhao, J.; Fang, W.; Xu, H. L. Sun, H. B. Unidirectional Lasing from a Spiral-Shaped Microcavity of Dye-Doped Polymers. *IEEE Photonics Technol. Lett.* **2015**, *27*, 311–314.
[19] Lin, J.; Xu, Y.; Tang, J.; Wang, N.; Song, J.; He, F.; Fang, W.; Cheng, Y. Fabrication of Three-Dimensional Microdisk Resonators in Calcium Fluoride by Femtosecond Laser Micromachining. *Appl. Phys. A* **2014**, *116*, 2019–2023.
[20] Lin, J.; Xu, Y.; Fang, Z.; Wang, M.; Wang, N.; Qiao, L.; Fang, W.; Cheng, Y. Second Harmonic Generation in a High-Q Lithium Niobate Microresonator Fabricated by Femtosecond Laser Micromachining. *Sci. China-Phys.* **2015**, *58*, 114209.
[21] Lin, J. T.; Xu, Y. X.; Fang, Z. W.; Wang, M.; Song, J. X.; Wang, N. W.; Qiao, L. L.; Fang, W.; Cheng, Y. Fabrication of High-Q Lithium Niobate Microresonators Using Femtosecond Laser Micromachining. *Sci. Rep.* **2015**, *5*, 8072.
[22] Wang, C.; Burek, M. J.; Lin, Z.; Atikian, H. A.; Venkataraman, V.; Huang, I. C.; Stark, P.; Lončar, M. Integrated High Quality Factor Lithium Niobate Microdisk Resonators. *Opt. Express* **2014**, *22*, 30924–30933.
[23] Wang, J.; Bo, F.; Wan, S.; Li, W. X.; Gao, F.; Li, J. J.; Zhang, G. Q.; Xu, J. J. High-Q Lithium Niobate Microdisk Resonators on a Chip for Efficient Electro-Optic Modulation. *Opt. Express* **2015**, *23*, 23072–23078.
[24] Lin, J. T.; Xu, Y. X.; Ni, J. L.; Wang, M.; Fang, Z. W.; Qiao, L. L.; Fang, W.; Cheng, Y.. Phase-Matched Second-Harmonic Generation in an On-Chip $LiNbO_3$ Microresonator. *Phys. Rev. Appl.* **2016**, *6*, 014002.

[25] Guarino, A.; Poberaj, G.; Rezzonico, D.; Degl'Innocenti, R.; Gunter, P. Electro-Optically Tunable Microring Resonators in Lithium Niobate. *Nat. Photon.* **2007**, *1*, 407–410.
[26] Wang, M.; Xu, Y.; Fang, Z.; Liao, Y.; Wang, P.; Chu, W.; Qiao, L.; Lin, J.; Fang, W.; Cheng, Y. On-Chip Electro-Optic Tuning of a Lithium Niobate Microresonator with Integrated In-Plane Microelectrodes. *Opt. Express* **2017**, *25*, 124–129.
[27] Fang, Z.; Xu, Y.; Wang, M.; Qiao, L.; Lin, J.; Fang, W.; Cheng, Y. Monolithic Integration of a Lithium Niobate Microresonator with a Free-Standing Waveguide Using Femtosecond Laser Assisted Ion Beam Writing. *Sci. Rep.* **2017**, *7*, 45610.
[28] Rosenberg, J.; Lin, Q.; Painter, O. Static and Dynamic Wavelength Routing Via the Gradient Optical Force. *Nat. Photon.* **2009**, *3*, 478–483.
[29] Lin, Q.; Rosenberg, J.; Jiang, X.; Vahala, K. J.; Painter, O. Mechanical Oscillation and Cooling Actuated by the Optical Gradient Force. *Phys. Rev. Lett.* **2009**, *103*, 103601.
[30] Wiederhecker, G. S.; Chen, L.; Gondarenko, A.; Lipson, M. Controlling Photonic Structures Using Optical Forces. *Nature* **2009**, *462*, 633–638.
[31] Van Thourhout, D.; Roels, J. Optomechanical Device Actuation Through the Optical Gradient Force. *Nat. Photon.* **2010**, *4*, 211–217.
[32] Jiang, X.; Lin, Q.; Rosenberg, J.; Vahala, K.; Painter, O. High-Q Double-Disk Microcavities for Cavity Optomechanics. *Opt. Express* **2009**, *17*, 20911–20919.
[33] Gorodetsky, M. L.; Pryamikov, A. D.; Ilchenko, V. S. Rayleigh Scattering in High-Q Microspheres. *J. Opt. Soc. Am. B* **2000**, *17*, 1051–1057.
[34] Dmitriev, V. G.; Gurzadyan, G. G.; Nikogosyan, D. N. *Handbook of Nonlinear Optical Crystals*; Springer - Verlag Berlin Heidelberg GmbH, 2013.
[35] Teraoka, I.; Arnold, S.; Vollmer, F. Perturbation Approach to Resonance Shifts of Whispering-Gallery Modes in a Dielectric Microsphere as a Probe of a Surrounding Medium. *J. Opt. Soc. Am. B* **2003**, *20*, 1937.
[36] Du, X.; Vincent, S.; Lu, T. Full-Vectorial Whispering-Gallery-Mode Cavity Analysis. *Opt. Express* **2013**, *21*, 22012.
[37] Du, X.; Vincent, S.; Faucher, M.; Picard, M. J.; Lu, T. Generalized Full-Vector Multi-Mode Matching Analysis of Whispering Gallery Microcavities. *Opt. Express* **2014**, *22*, 13507.